Project report: Phase analysis of an additive manufactured intermetallic titanium aluminide alloy using synchrotron radiation

Malina Jop

Montanuniversität Leoben, Leoben, Austria

Supervisor: Dr. Peter Staron

Helmholtz-Zentrum Geesthacht

DESY Summer Student Programme 2018

Hamburg, 05.09.2018

Abstract

In search of new advanced engineering materials intermetallic titanium aluminides alloys attract increasing interest of researchers for their combination of low density and outstanding mechanical properties - especially at elevated temperatures - which makes them suitable for high temperature application like aircraft turbine blades, automotive engines and turbocharger wheels, being a viable option to replace weighty nickel-based superalloys. During the electron beam melting (EBM) process, titanium aluminide powder is additively manufactured layer by layer into an almost void free and dense engineering part. The EBM process effects the microstructure and the occurring fractions of different titanium aluminide phases. As the properties of the alloy are mostly determined by the phases present and their distribution, it is highly relevant to understand how the composition of the material changes during additive manufacturing. The aim of this report is to give a brief overview of the phase analysis of two EMB processed titanium aluminide alloy samples using synchrotron radiation from PETRA III at the Deutsches Elektronen Synchrotron (DESY), Hamburg, Germany. The analysis was conducted in the research group of Helmholtz Zentrum Geesthacht (HZG) during the months of July and August 2018 as part of the DESY Summer Students Programme 2018.

Table of contents

1 Introduction

Intermetallic titanium aluminide alloys show outstanding mechanical properties, especially at elevated temperatures, which makes them suitable for high temperature application like aircraft turbine blades, automotive engines and turbocharger wheels. In contrast to other alloys used in high temperature applications, titanium aluminide alloys are very lightweight with a density of about 4,0 gcm^{-3} which makes them a viable option to replace weighty nickel-based superalloys.[1] The two samples studied in this project consist of an intermetallic titanium aluminide alloy with a composition of almost equal atomic parts of titanium and aluminium, combined with a total of 4 at.% of other alloying elements. This γ-TiAl based alloy is a so-called 2nd generation alloy that mainly consists of γ-TiAl phase ($L1_0$ crystal structure) and a small volume fraction of α_2-Ti_3Al ($D0_{19}$ crystal structure) at room temperature.

Both samples studied for this report were additively manufactured into a solid part using electron beam melting (EBM). During the EMB process alloy powder is spread out on a work bench in thin layers and then successively melted by the heat generated by a concentrated electron beam. This technique allows building up complex geometry engineering parts near-net-shape.[2]

Sample 1 was analysed after the EBM process with no further treatment, sample 2 was hot isostatically pressed (HIPed) after the EBM process. Metallographic sections parallel to the building directions were prepared and studied under a scanning electron microscope (SEM) using the viewing direction shown in Figure 1.

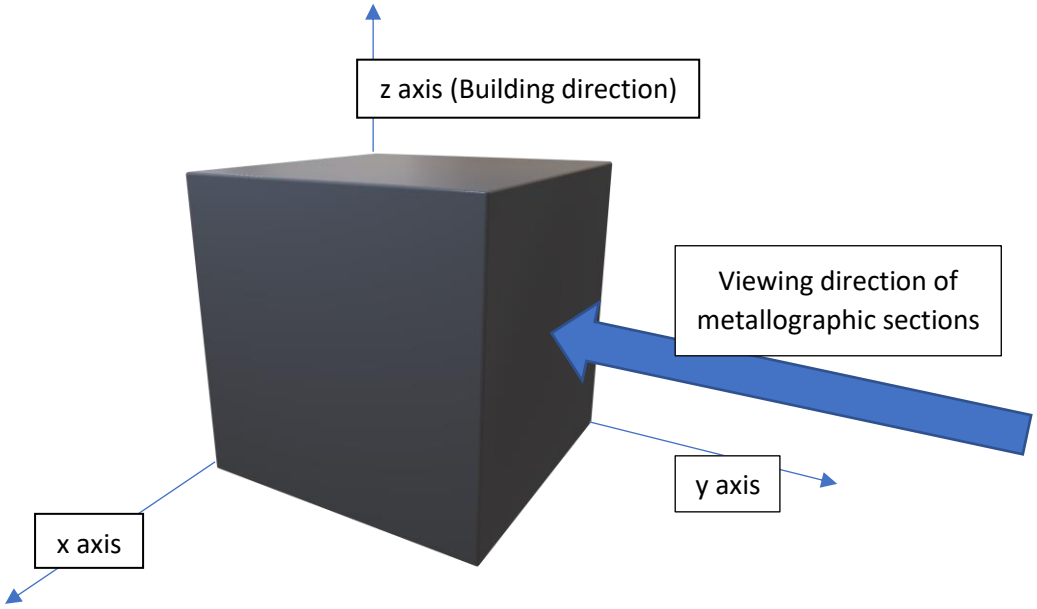

Figure 1: Visualisation of the viewing direction in metallographic sections.

Images depicting the microstructure of both samples are given in Figures 2 to 5.

[1] S. Mayer, P. Erdely, F.D. Fischer, D. Holec, M. Kastenhuber, T. Klein, H. Clemens, *Intermetallic β-solidifying γ-TiAl based alloys – from fundamental research to application*, Advanced Engineering Materials 2017, 19, No. 4.
[2] S. Biamino, A. Penna, U. Ackelid, S. Sabbadini, O. Tassa, P. Fino, M. Pavese, P. Gennaro, C. Badini, *Intermetallics* 2011, 19, 776; G. Baudana, S. Biamino, B. Klöden, A. Kirchner, T.Weißgärber, B. Kieback, M. Pavese, D. Ugues, P. Fino, C. Badini, *Intermetallics* 2016, 73, 43.

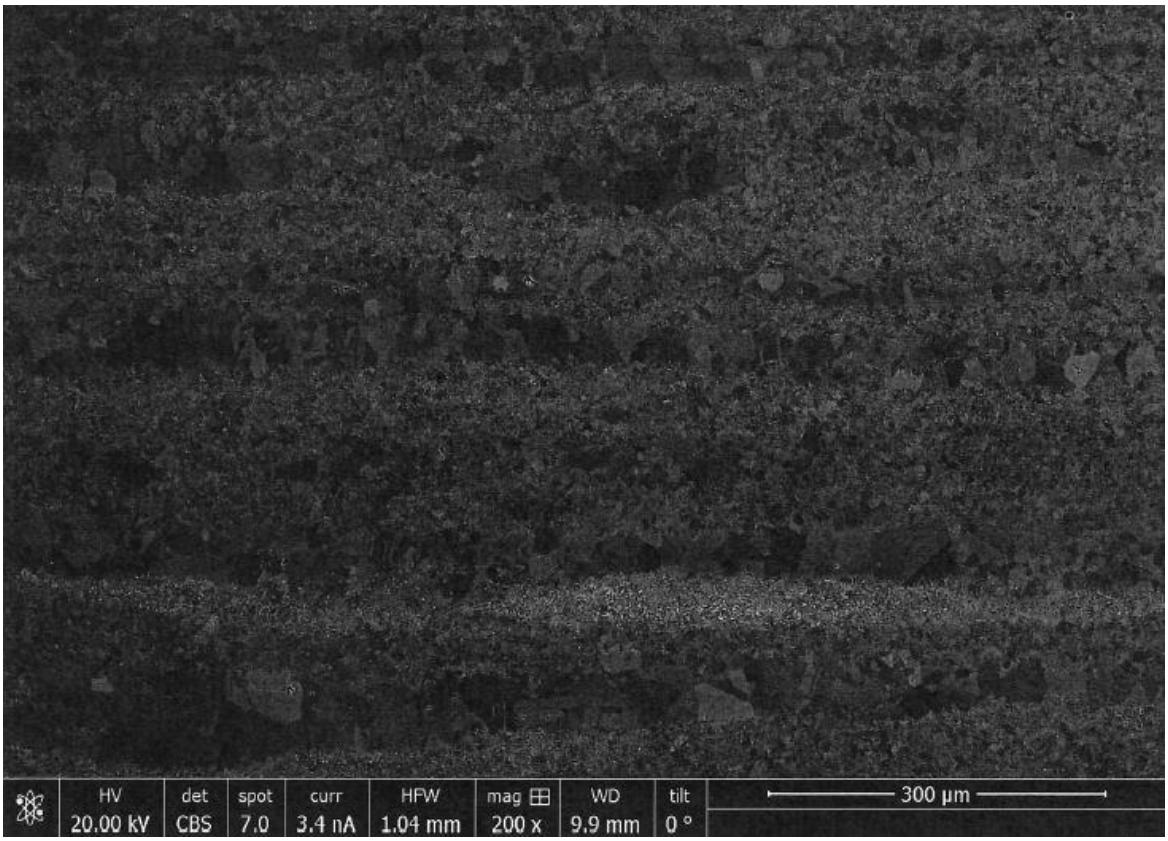

Figure 2: Sample 1 (as-EBM condition) SEM image of microstructure taken in back-scattered electron (BSE) mode.

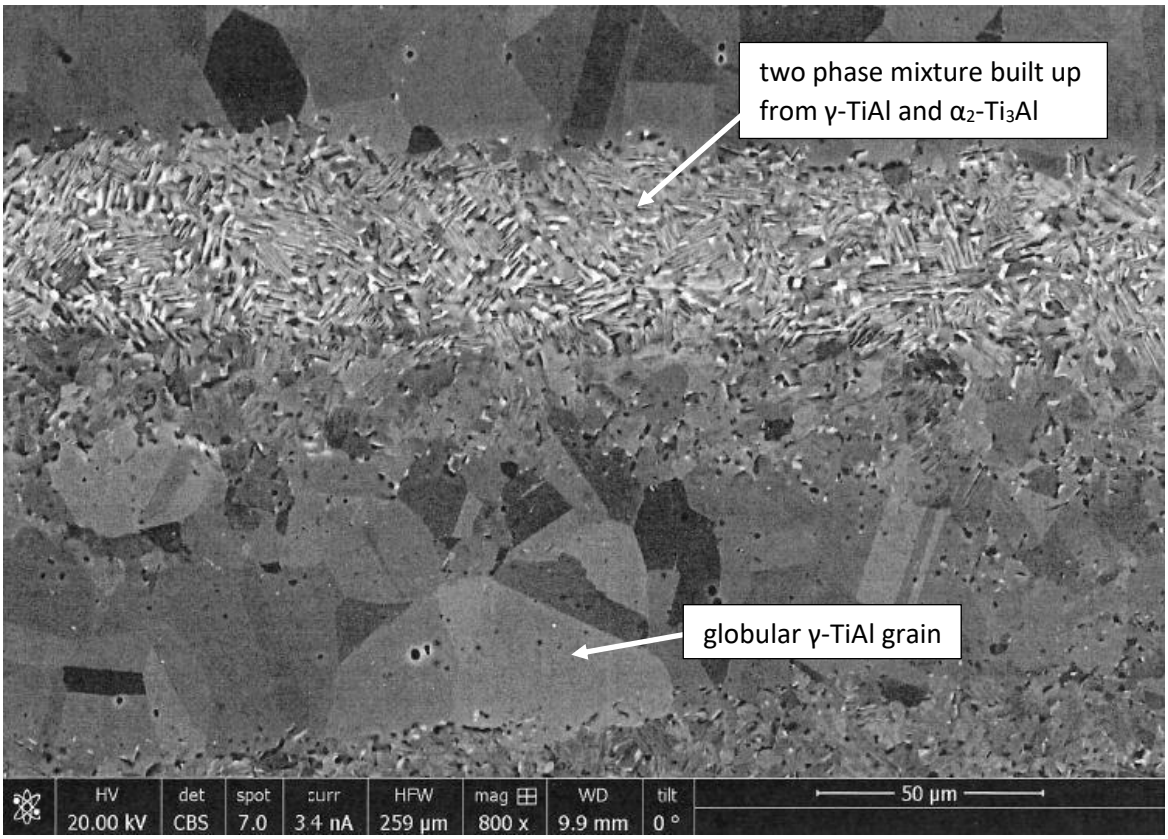

Figure 3: Sample 1 (as-EBM condition) SEM image of microstructure in BSE mode, higher magnification.

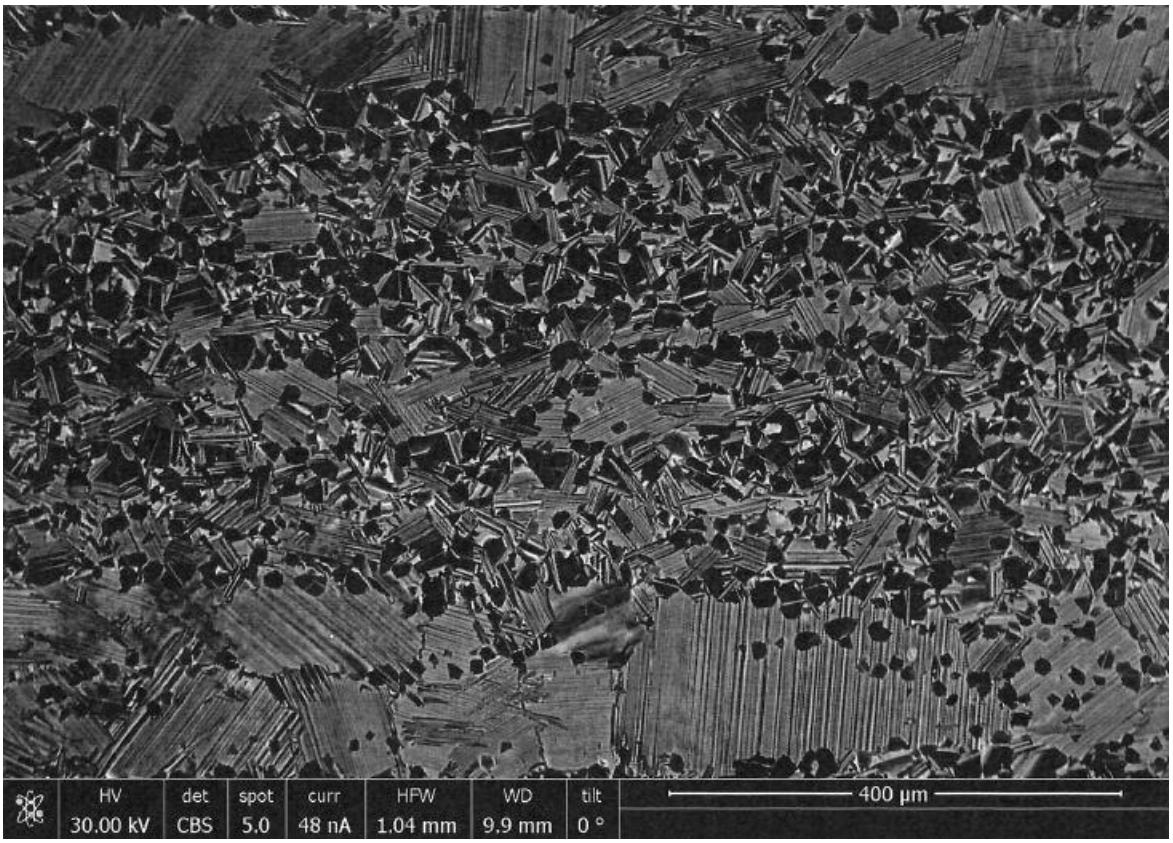

Figure 4: Sample 2 (HIPed condition) SEM image of microstructure in BSE mode.

Due to the HIP process coarse γ/α_2–colonies have formed.

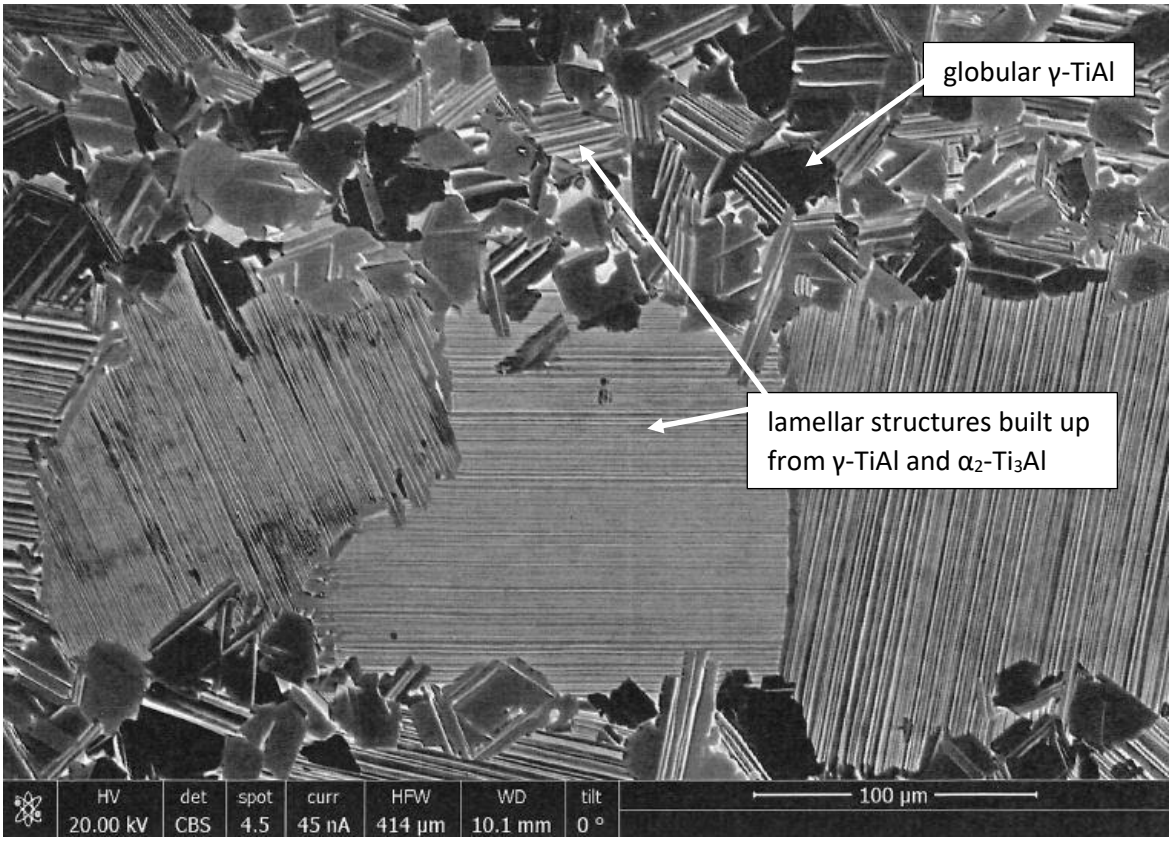

Figure 5: Sample 2 (HIPed condition) SEM image of microstructure in BSE mode, higher magnification.

The metallographic sections show a layered two–phase microstructure with layer thickness ranging from 20 µm to up to 150 µm. The phases occurring in the layers are colonies of globular γ-TiAl grains and regions of lamellar structures built up from α_2-Ti_3Al and γ-TiAl phase. γ-TiAl has a tetragonal distorted face-centred cubic cell that, depending on alloy concentration, processing and heat-treatment history, contains 48 at.% to 65 at.% percent of aluminium, α_2-Ti_3Al is ordered hexagonally structured with an aluminium content between 22 at.% and 39 at.%.[3] A third phase, body-centred cubic β_0-TiAl, could be present in traces, but no visible regions have been found in the samples.

The layered microstructure could be explained as a consequence of the EBM process which causes aluminium to locally evaporate, leading to the formation of aluminium poorer α_2-Ti_3Al phase. The materials mechanical properties, workability and other characteristics are heavily impacted by the phases and the phase distribution within the sample, thus it is of major interest to understand and analyse the microstructural arrangement of phases. In case of these two additive manufactured samples the main focus of interest is on the phase distribution with respect to building direction (z-axis position, see Figure 1).

2 Experimental set up and measurement

2.1 Theoretical background

When an x-ray beam irradiates a polycrystalline sample, x-rays diffract on planes that satisfy Braggs law (Figure 6). As different phases have different crystal structure, i.e. planes and lattice parameters, the phases create characteristic cone-shaped diffraction patterns, so-called Debye-Scherrer rings, that are recorded on a 2-dimensional detector. The plane and therefore the phase from which the photons were diffracted can be retraced by measuring the 2θ angle. The volume phase fraction present in the sample can also be evaluated from the diffraction data.

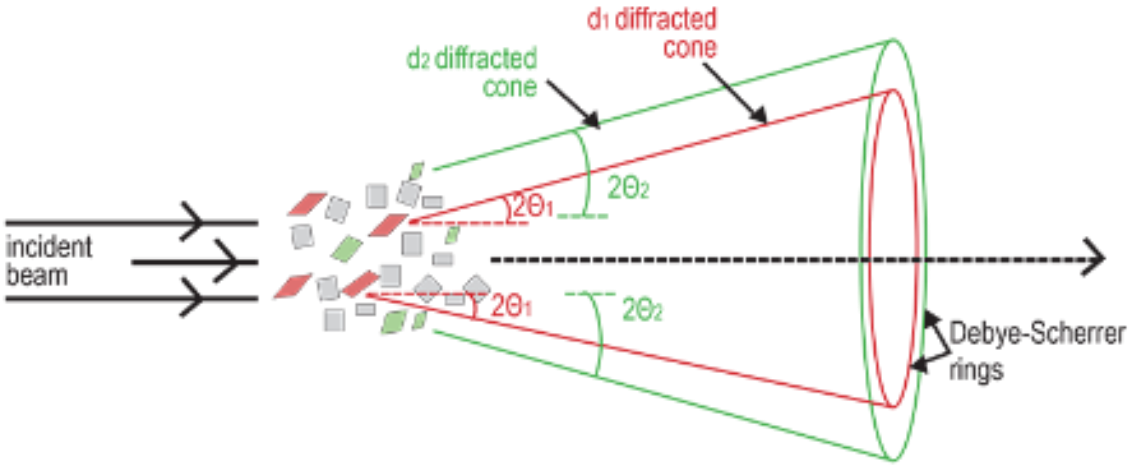

Figure 6: Schematic representation of x-ray diffraction in polycrystalline materials[4]

[3]H. Clemens, S. Mayer, *Design, Processing, Microstructure, Properties, and Applications of Advanced Intermetallic TiAl Alloys*, Advanced Engineering Materials 2013, 15, No. 4.

[4]https://www.diamond.ac.uk/industry/Industry-News/Latest-News/Synchrotron-Industry-News-Advent-Calendar-2016/Day-10-and-11---Powder-Diffraction.html, last accessed 23.08.2018

2.2 Sample preparation and measurement parameters

In order to quantitively study the volume fraction of γ-TiAl and α_2-Ti_3Al occurring in each layer, the two samples were cut into cuboids and prepared for an x-ray diffraction experiment in transmission mode using synchrotron radiation (See Figure 7). The width of the cuboid being screened was chosen to be 4mm in order to get a signal with balanced absorption and diffraction intensity.

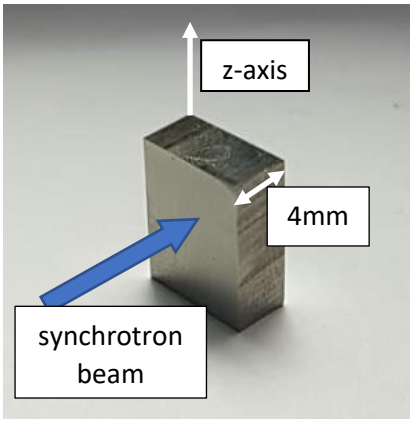

Figure 7: Cuboid cut out from original sample

All measurements were conducted at the test facility EH1 beamline P07, the so-called *High Energy Materials Science Beamline of Helmholtz-Zentrum Geesthacht (HZG) and DESY* at PETRA III. The photon energy used for measurement was E=87.1 keV, which corresponds to a wavelength of λ=0,14236 Å. The beam was centred in middle of the sample and focused on a spot size of 700 µm (horizontal) and 10 µm (vertical) and was then gradually moved along the z-axis with a step size of 5 µm and exposure time of 40 seconds (2 seconds x 20 frames). A total distance of 500 µm along the building direction was screened from top to bottom in transmission mode. According to the metallographic sections given in Figures 2 to 5 the typical layer size is apparent to be between 20 µm and 150 µm. Therefore, the screened line along the z-axis should traverse at least three distinguishable layers of globular γ-TiAl and lamellar γ-TiAl and α_2-Ti_3Al.

3 Data analysis

3.1 Debye-Scherrer rings

Diffraction patterns of sample 1 and sample 2 in the first z-position are shown in Figures 8 and 9.

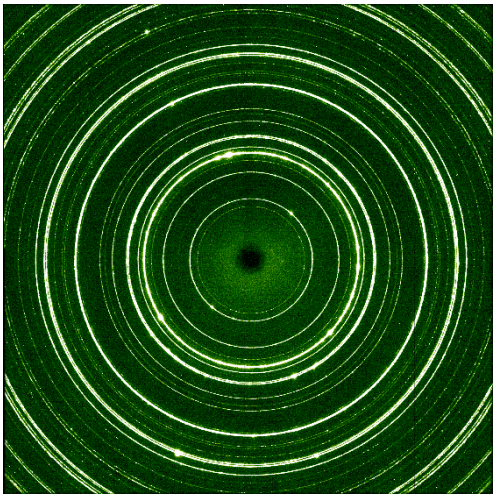

Figure 8: Debye-Scherrer ring of sample 1

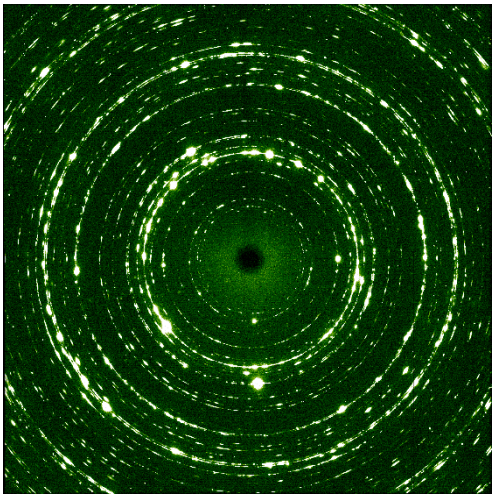

Figure 9: Debye-Scherrer Ring of sample 2

On a first view and before quantitative phase analysis is conducted, a few conclusions about the samples can be made just by examining the diffraction rings visually:

It becomes immediately evident that sample 1 creates a smoother and more continuous ring, while the diffraction pattern of sample 2 appears speckled and spotty. This can be explained by a larger average grain size of the crystallites (grains) in sample 2 which is in accordance with the metallographic sections shown in Figures 4 and 5. Some spots presumably originating from diffraction of an above average sized γ-TiAl grain can also be seen in the Debye-Scherrer rings arising from sample 1.

The samples seem to be texture-free and without preferred grain orientation which can be concluded from uniform intensity of the Debye-Scherrer rings in all directions of space.

In Figure 10 the following planes in γ-TiAl and α_2-Ti_3Al phases are assigned to a certain Debye-Scherrer ring. However, there are no signs of diffraction rings caused by body-centred cubic β_0 phase.

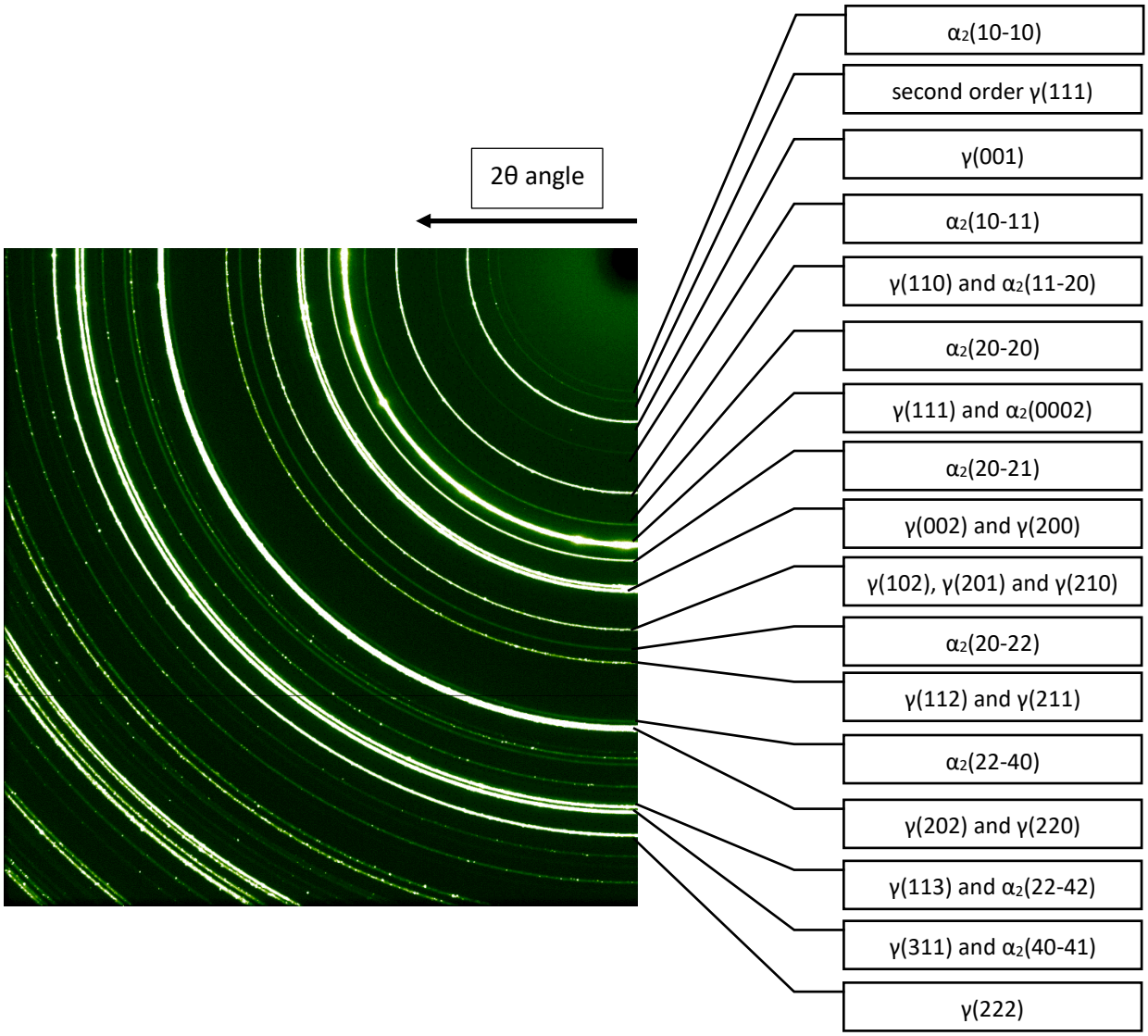

Figure 10: Assigned phases and planes for Debye-Scherrer rings appearing in the investigated γ-TiAl based alloy which consists of γ-TiAl and α_2-Ti_3Al phase.

3.2 Rietveld refinement with *Maud*

Diffraction rings were measured for every z-position, resulting in 100 Debye-Scherrer rings for each sample. The software *Fit2D* was used to convert the visual detector data to numerical datasets by evaluating the intensity measured by the detector as a function of the Debye-Scherrer ring radius, which is proportional to the 2θ angle of each reflex. For analysis the whole circle extent of 360° was used by integrating the intensity values around the circle at a given radius. This leads to a dataset with values for the intensity as a function of 2θ angle.

As the diffraction data can be used to quantitatively interpret the volume fractions of the phases present, a Rietveld analysis was carried out by using the software *Maud*, see Figure 11. Rietveld analysis is a method which applies a theoretical model and fits the measured data. Variable parameters are then refined by iterating calculations of the discrepancy between model and theory by a least-square approach after each fitting process.[5] In this refinement, models of the three phases γ, α_2 and β_0 were used to fit the measured data. The theoretical data progression resulting from the models can be seen as a red line in Figure 11. Circles mark measured data, small vertical lines under the plot indicate the phase that creates the peak above. The white bar underneath indicates the difference between measured and theoretical data. With every iteration process, parameter like full width at half maximum (FWHM), volume fraction, crystallite size etc. are refined to minimize the error and fit the red line more precisely.

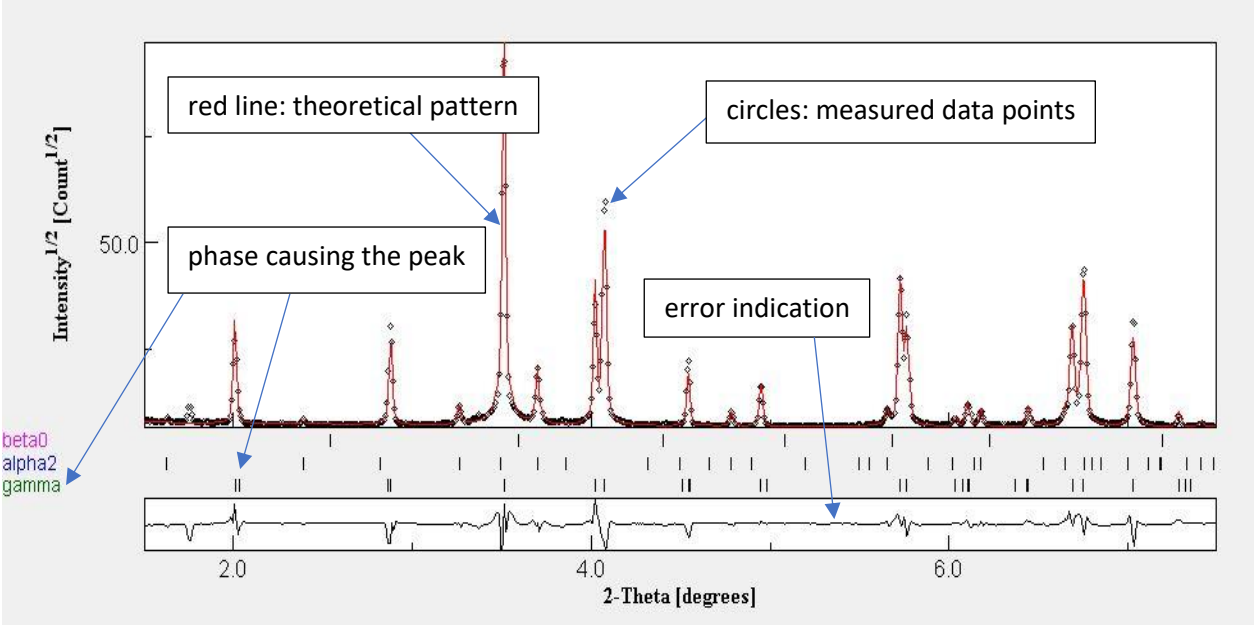

Figure 11: Screenshot from a Rietveld analysis using the software Maud (see text).

Rietveld refinement has been conducted for every z-position. According to expectations, one should see changes in volume fractions of phases with respect to the z-axis as the measured line traverses layers of different composition.

Results from Rietveld refinement for the volume fraction of phases as a function of z-position for sample 1 and sample 2 are given in Figures 12 and 13.

[5]Rietveld, H. M. (1969): *A profile refinement method for nuclear and magnetic structures*. Journal of Applied Crystallography, 2(2), 65–71.

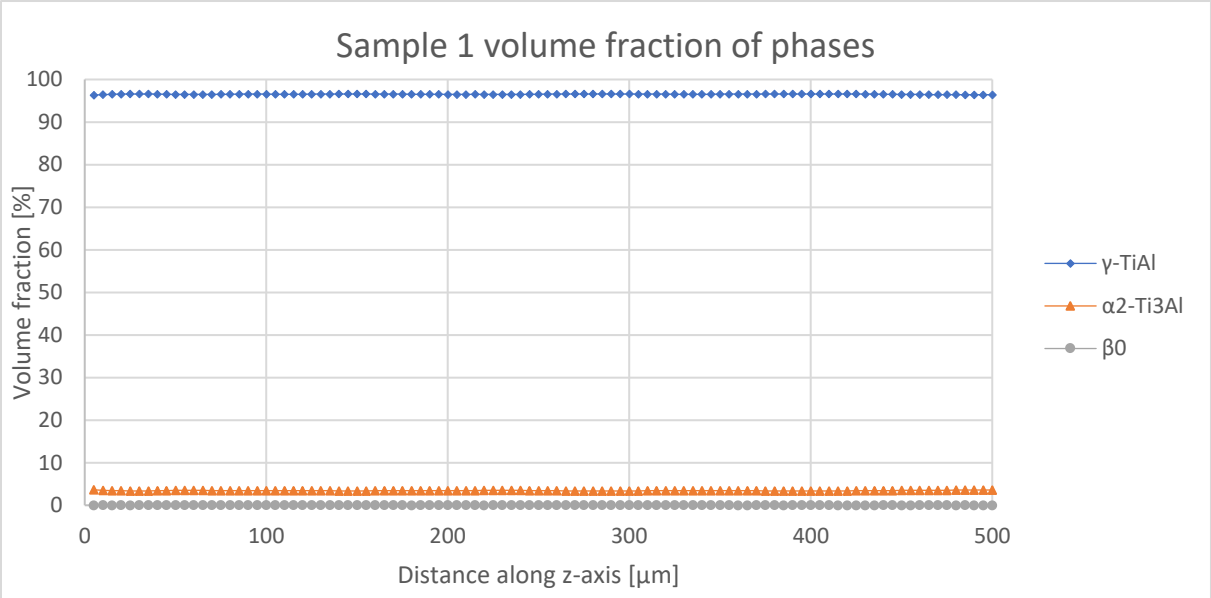

Figure 12: Rietveld analysis for sample 1 using Maud.

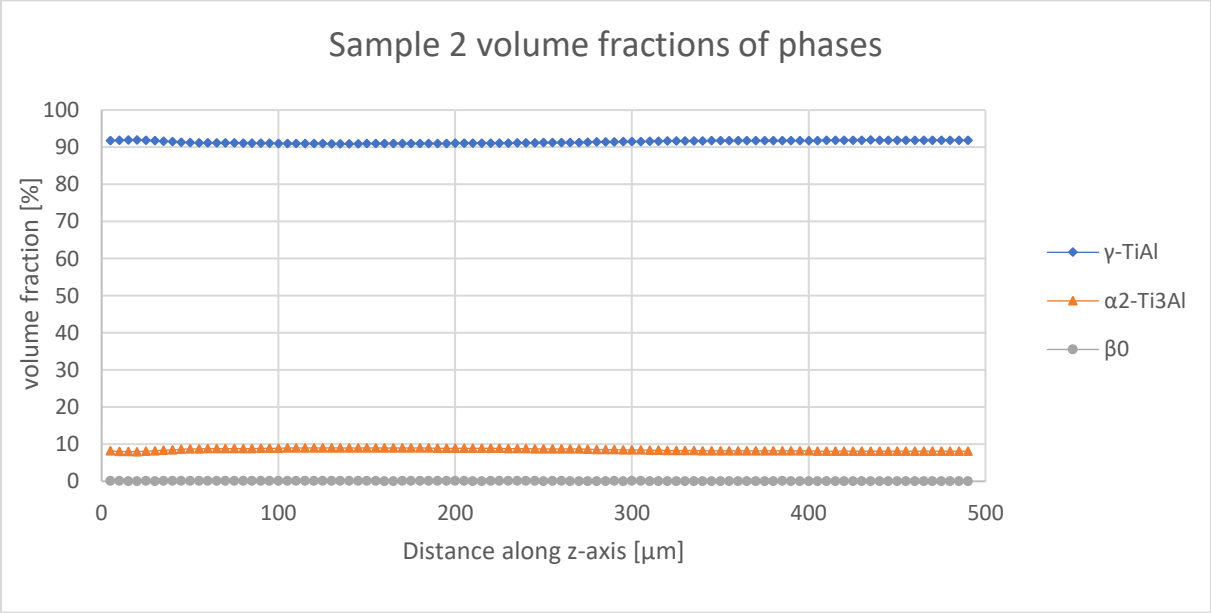

Figure 13: Rietveld analysis for sample 2 using Maud.

On a large scale the measured phase fractions appear to be constant with respect to the z-axis and the expected oscillation from α_2-Ti_3Al richer regions compared to layers containing only globular γ-TiAl grains are not observed. The result for the maximum volume fraction of β_0 is below 0.01 vol.%, thus this phase is neglected in further analysis due to a lack of relevance in these samples.

By scaling up the results from Rietveld analysis and putting the rarer α_2-Ti_3Al phase on the second y-axis, the following results are obtained (Figure 14 and 15).

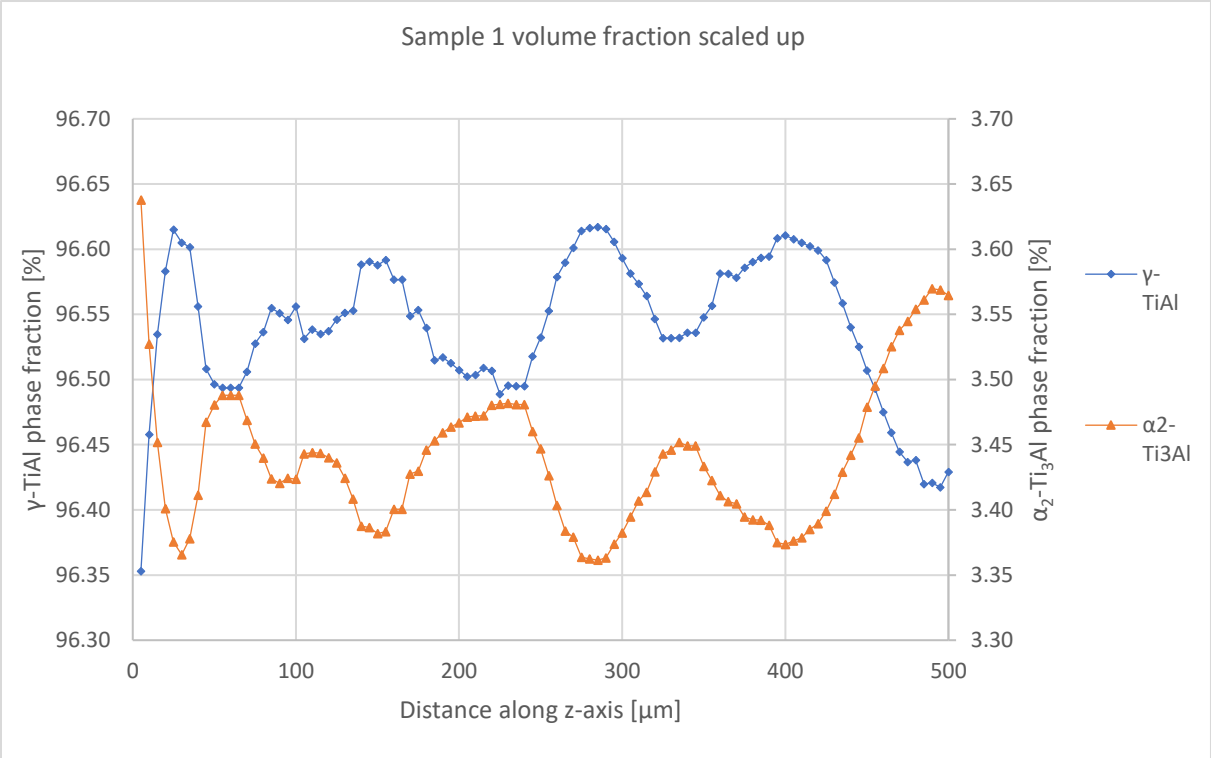

Figure 14: Sample 1 with scaled up volume fractions.

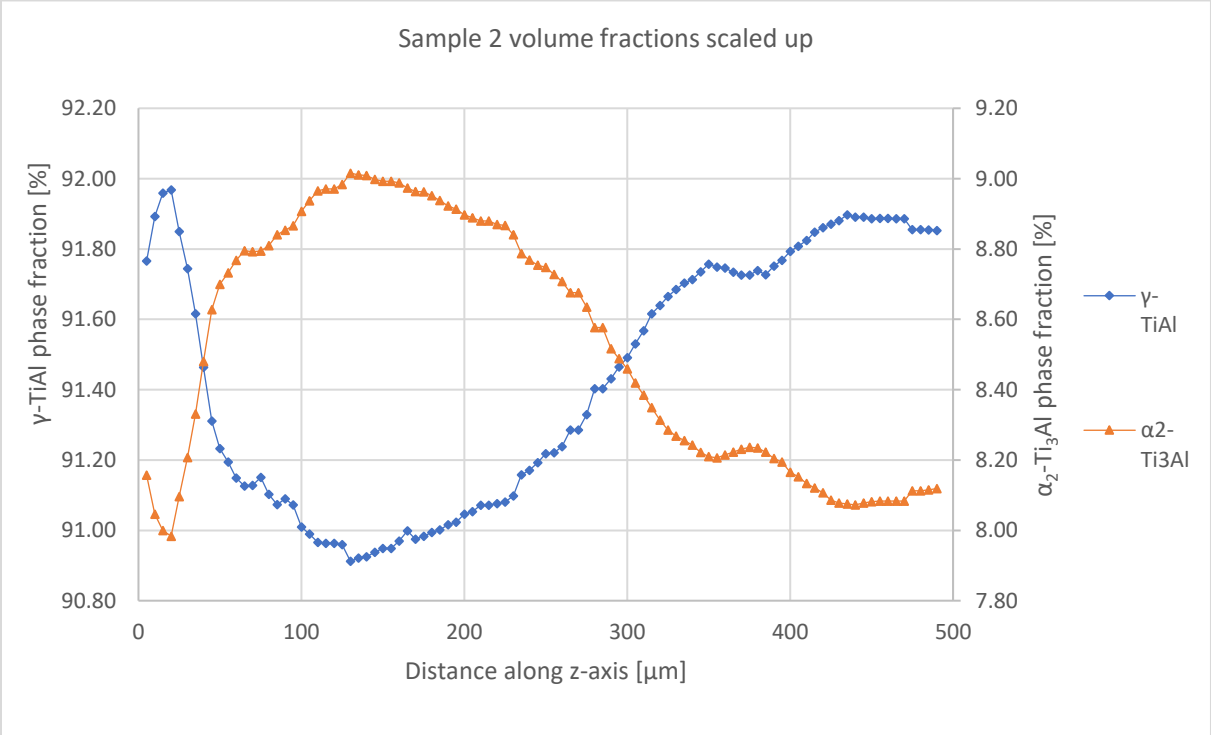

Figure 15: Sample 2 with scaled up volume fractions.

When scaled up, small oscillations can be noticed. Distances from peak to peak in the oscillation from sample 1 can be correlated to the average layer thickness as seen in the SEM images of the microstructure in Figures 2 and 3. The Rietveld analysis for sample 2 appears to cover only 1.5 layers over the measuring length of 500 µm. Regarding the outcome of the Rietveld analysis in Figure 15 the measured layer has a vertical spatial extent of about 250 µm. Such a wide layer has not been observed when analysing the microstructure prior to the synchrotron measurement, nonetheless it is not impossible. To clarify this issue a metallographic section of the samples will be made, and the exact path covered by the photon beam will be reconstructed in order to see if there is indeed a layer of 250 µm as predicted by the synchrotron measurement.

During Rietveld analysis not only the volume fraction was fitted, but also other variable parameters, i.e. the crystallite (grain) size. As γ-TiAl exists in both, lamellar and globular regions with different average grain sizes, an error could occur as Maud evaluated only one uniform crystallite size during the analysis conducted in this project. To solve this problem, another approach will be made that allows to fit two separated and independent crystallite sizes for γ-TiAl.

3.3 Peak integrals with *Afit*

Because the recorded change in volume fractions derived by Rietveld refinement unfolds in a range of under 1 %, another method was conducted to cross-check the results. In an intensity-2θ scan, the area under a peak assigned to a phase is proportional to the volume fraction of that phase in the sample. As seen in Figure 11, some peaks overlap and as only peaks that are assigned to solely one phase are suitable for this analysis, certain peaks were chosen and their peak integral was plotted with respect to the distance on the z-axis. According to expectations, one should be able to see the same oscillation as in the scaled-up chart from the rietveld analysis. The software *Afit* was used to calculate the peak integrals.

The peaks chosen for γ-TiAl are (001), (112) and the doublepeak (002) and (200).

The peaks chosen for α_2-Ti_3Al are (20-20), (20-21) and (20-22).

In Figures 16 and 17 the sum of the peak integrals for each phase in sample 1 and 2 is depicted.

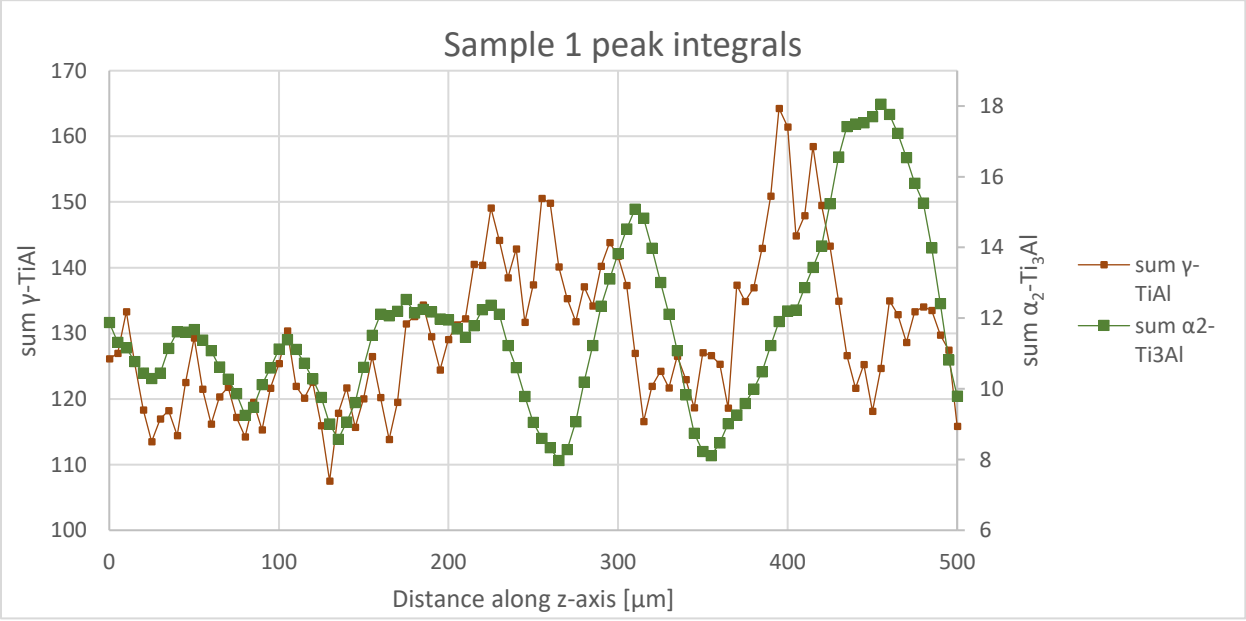

Figure 16: Sample 1: sum of peak integrals for the chosen γ-TiAl and α_2-Ti_3Al peaks (see text).

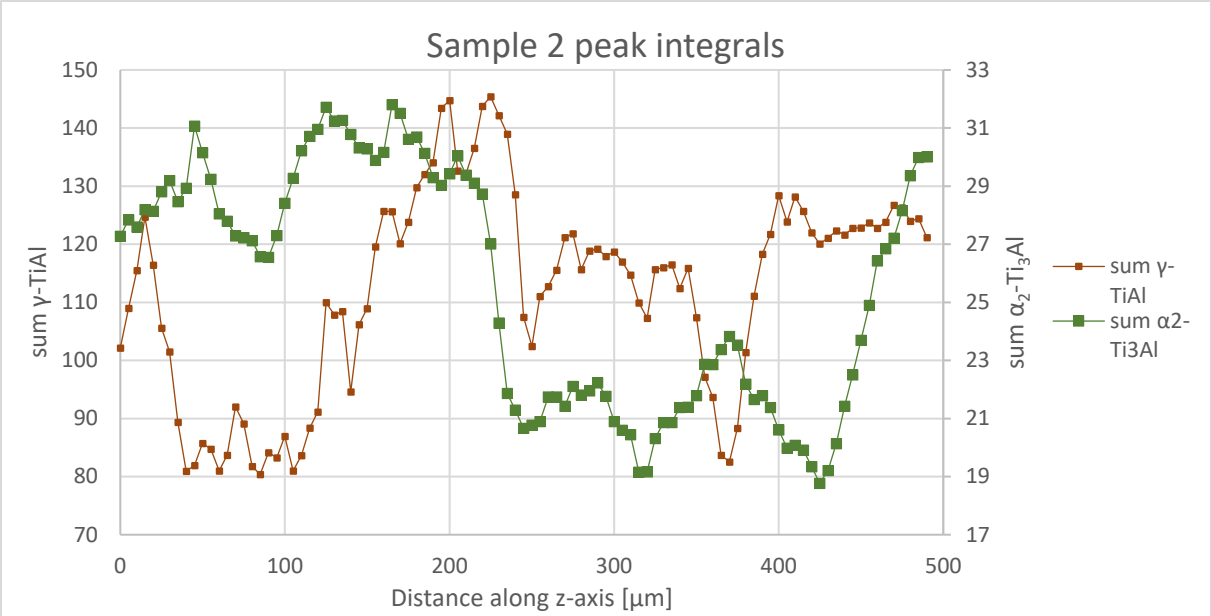

Figure 17: Sample 2: sum of peak integrals for the chosen γ-TiAl and α_2-Ti_3Al peaks (see text).

When compared to the Rietveld analysis, it becomes evident that they do not show the same oscillating behaviour. It is not well understood yet, why the sum of peak integrals for γ-TiAl and α_2-Ti_3Al phases do not show mirrored pathways and why they are not in accordance with the outcome of the Rietveld analysis.

Plots containing only peak integrals of either γ-TiAl or α_2-Ti_3Al phase raise further questions (Figures 18 to 21). It is also not understood, why the peak integrals of different planes from the same phase appear mirrored and, in addition, party exhibit opposed behaviour.

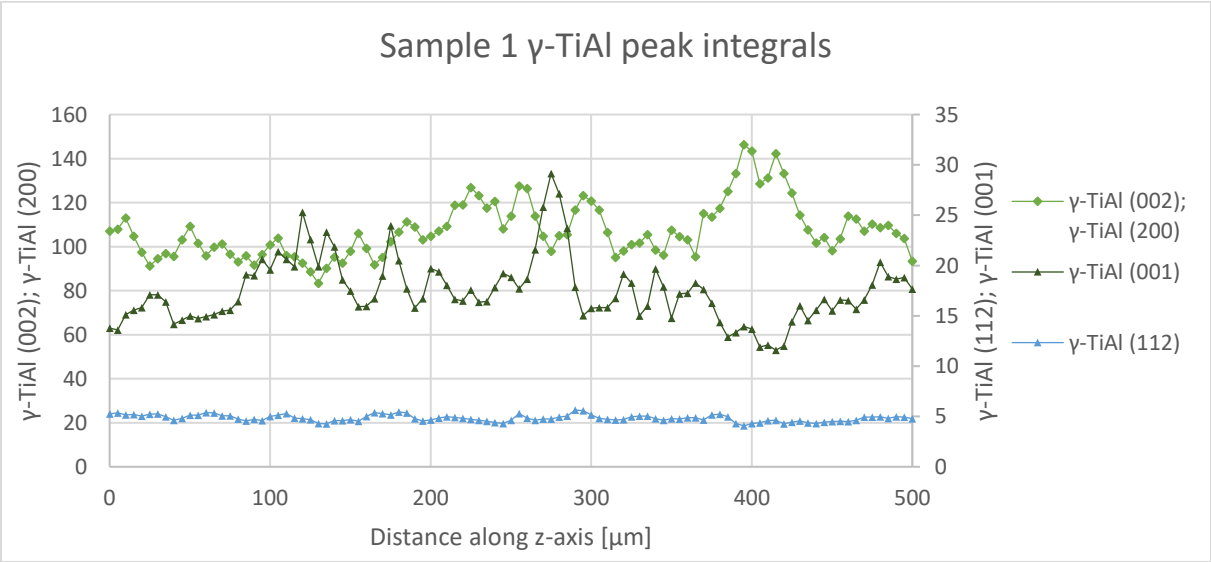

Figure 18: γ-TiAl peak integrals of sample 1.

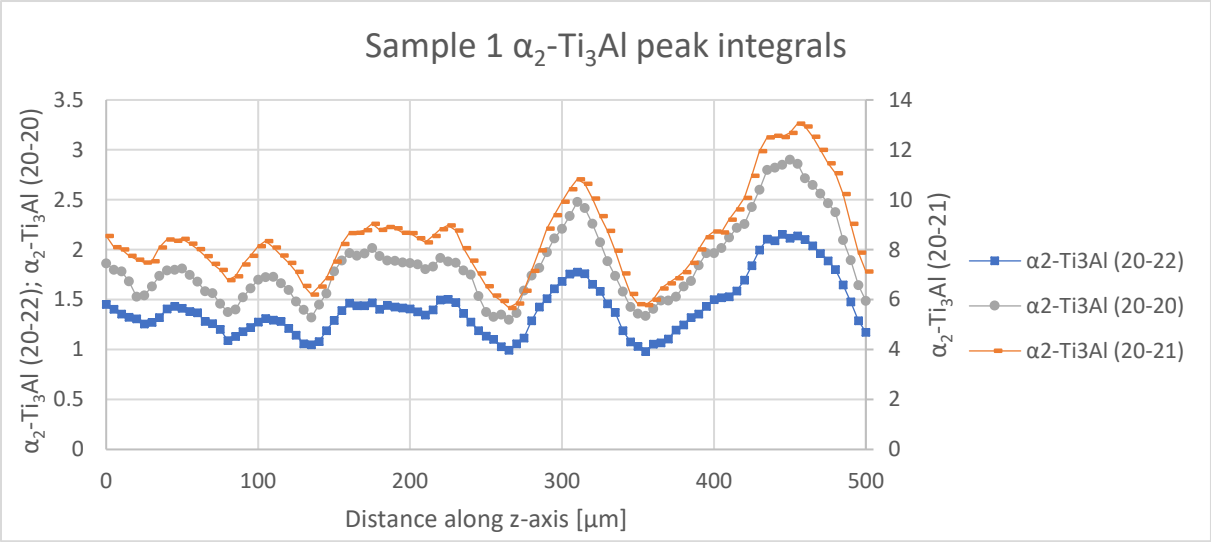

Figure 19: α_2-Ti_3Al peak integrals of sample 1.

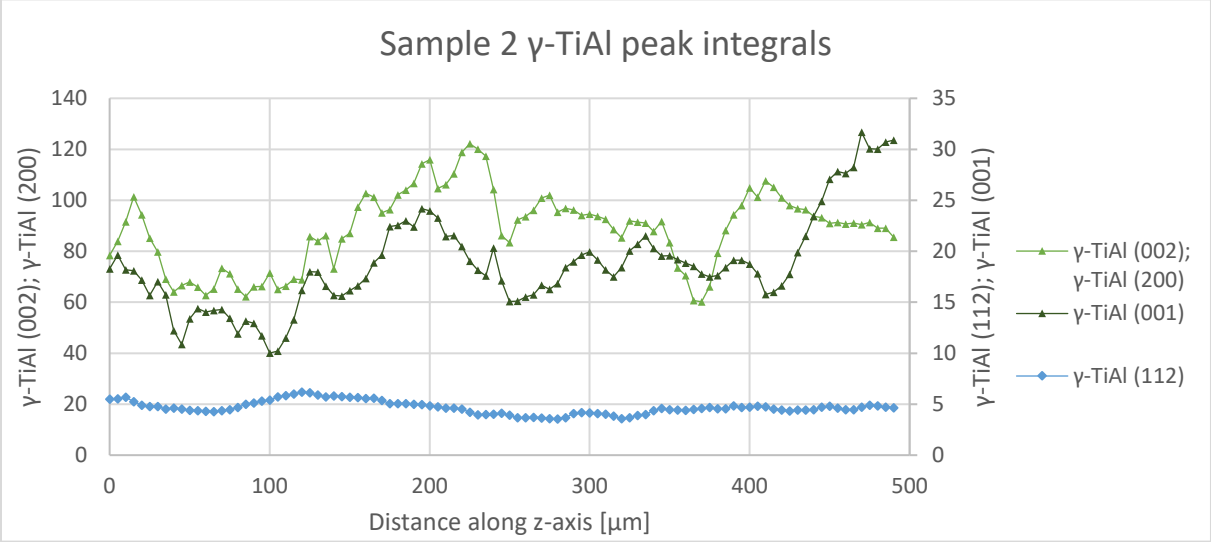

Figure 20: γ-TiAl peak integrals of sample 2.

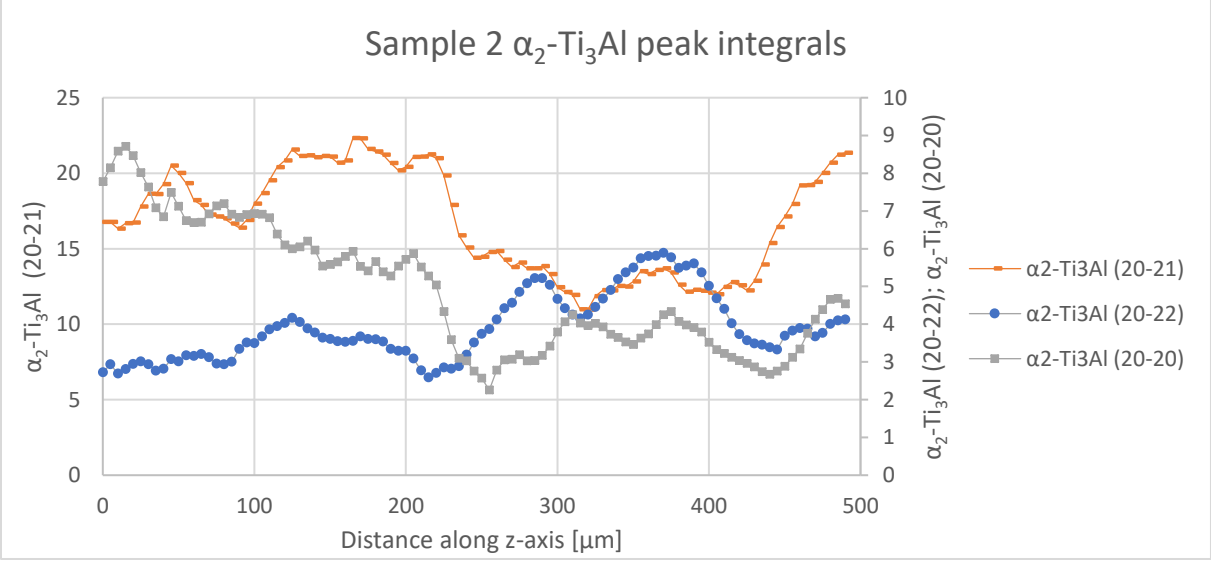

Figure 21: α_2-Ti_3Al peak integrals of sample 2.

3.4 Phase analysis with laboratory XRD

To obtain further information on phase distribution within the samples, an XRD scan with a laboratory x-ray source has been conducted. The beam was focused to a spot size of 4 mm (horizontal) and 50 µm (vertical) and then moved along the z-axis in 50 µm steps after each 2θ /omega-scan. With this technique only surface-near regions of samples are measured which should reflect the microstructure shown in the metallographic cuts (Figures 2 to 5).

As seen in Figure 22 the only visible α_2-Ti_3Al peak is the α_2(20-21) reflex. The peak is very weak when compared to the dominant γ-TiAl phase peaks. This did not change when the beam was moved along the z-axis or in case of sample 2. For this reason, it assumed that this particular XRD set up used in this experiment is not suitable for quantitative phase analysis desired for these samples.

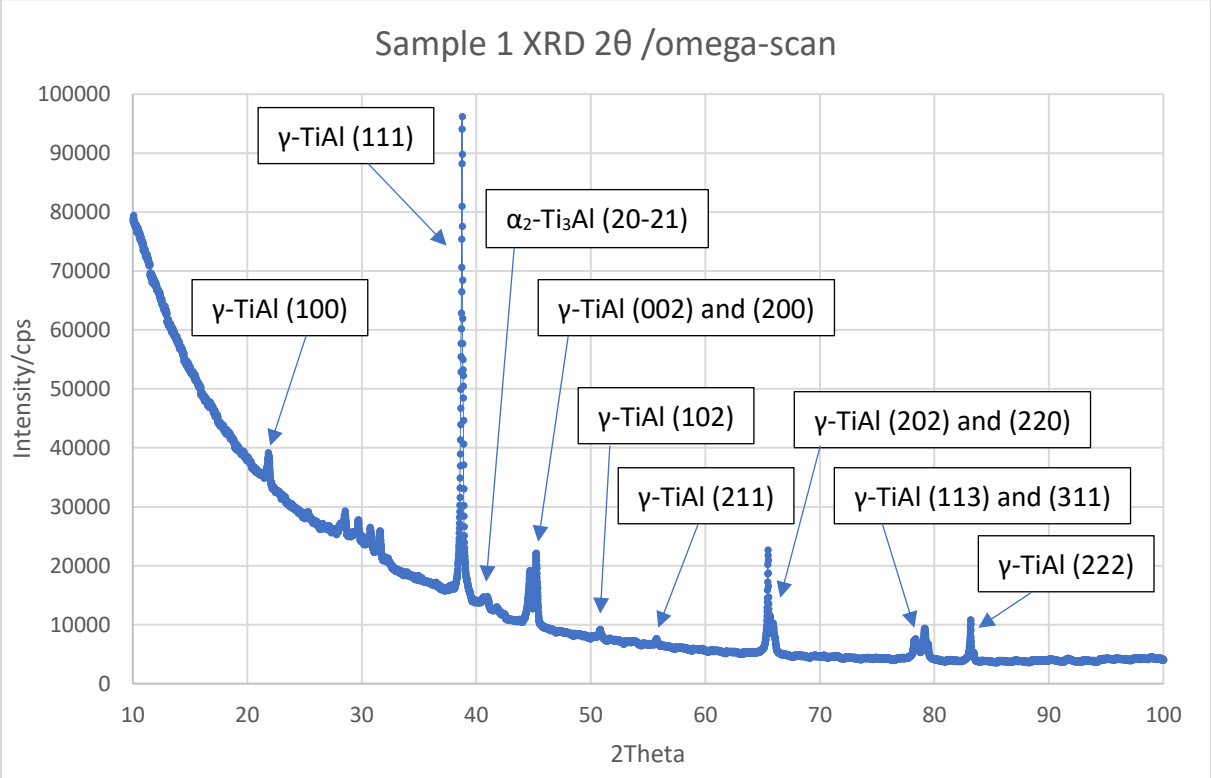

Figure 22: Representative XRD scan

4 Conclusion and outlook

The main conclusion which can be drawn from this fascinating summer research project is that phase analysis of additive manufactured titanium aluminide alloys is more complex and difficult than expected.

In total, the high proportion of γ-TiAl phase as seen in Figures 12 and 13 makes sense as the alloy contains a high aluminium content which stabilizes the γ-TiAl phase. Thus, the content of 80 vol.% to up to 97 vol.% of γ-TiAl seems reasonable. A possible explanation for the low measured phase difference with respect to the z-axis when analysing with *Maud*/Rietveld refinement could be inhomogeneous layer thickness as well as process-related chemical fluctuations. The photon beam passes through a 4 mm thick sample and the possibility of measuring through multiple layers is likely because of the local inhomogeneous layer distribution (see Figures 2 to 4). To solve this potential problem, another measurement will be conducted on the same sample using only a 500 µm thick

specimen to increase the probability of only measuring through only one layer at once. Changes in volume fractions should be better measurable then.

As seen in Figure 13, where only 1.5 oscillations of layers have been measured over the measuring length of 500 µm. This suggests that a longer distance along the z-axis should be measured in order to get a statistically more relevant result.

Metallographic examinations will be made in the region where the synchrotron measurement has been conducted, so measured layers can be correlated and optically identified in order to validate the measured data.

Why peak integrals are not in accordance with the Rietveld analysis and why some diffraction planes of the same phase exhibit opposed behaviour will be studied in more detail in a following project proposed by the Montanuniversität Leoben, Austria.

Phase analysis of additive manufactured titanium aluminides is still an ongoing research project that requires further devoted research work using more homogenius specimens processed with optimized EBM parameters. The objective of this project report is to only give an overview of the findings so far during the DESY Summer Student Programme 2018.

Acknowledgment

I would like to thank my supervisor Dr. Peter Staron from Helmholtz Zentrum Gesthacht (HZG) and the whole HZG group for warmly incorporating me and all their time spent on patiently giving first hands-on experiences and insights in the world of synchrotron radiaton for materials science. More over I would like to thank Dr. Emad Maawad for conducting the measurents at the beamline and explaining all the software used for analysis to me and Dr. Dieter Lott for introducing me to the laboratory XRD facility.

I am also very grateful for many fruitful discussions on titanium almuminides and ongoing support throughout my studies by Prof. Helmut Clemens, Prof. Svea Mayer and DI Reinhold Wartbichler (all Montanuniversity Leoben, Austria).

Very special thanks are owed to the whole DESY Summer Student Programme 2018 organisation team that made this unique opportunity possible!